Meteoritics & Planetary Science 40, Nr 9/10, 1393–1411 (2005)
Abstract available online at http://meteoritics.org

Ejection of Martian meteorites

Jörg FRITZ[1*], Natalia ARTEMIEVA[2], and Ansgar GRESHAKE[1]

[1]Institut für Mineralogie, Museum für Naturkunde, Humboldt-Universität zu Berlin, Invalidenstrasse 43, 10115 Berlin, Germany
[2]Institute for Dynamics of Geospheres, Russian Academy of Science, Leninsky Prospect 38, Building 1, Moscow 119334, Russia
[*]Corresponding author. E-mail: joerg.fritz.1@rz.hu-berlin.de

(Received 29 March 2005; revision accepted 11 April 2005)

Abstract–We investigated the transfer of meteorites from Mars to Earth with a combined mineralogical and numerical approach. We used quantitative shock pressure barometry and thermodynamic calculations of post-shock temperatures to constrain the pressure/temperature conditions for the ejection of Martian meteorites. The results show that shock pressures allowing the ejection of Martian meteorites range from 5 to 55 GPa, with corresponding post-shock temperature elevations of 10 to about 1000 °C. With respect to shock pressures and post-shock temperatures, an ejection of potentially viable organisms in Martian surface rocks seems possible. A calculation of the cooling time in space for the most highly shocked Martian meteorite Allan Hills (ALH) 77005 was performed and yielded a best-fit for a post-shock temperature of 1000 °C and a meteoroid size of 0.4 to 0.6 m. The final burial depths of the sub-volcanic to volcanic Martian rocks as indicated by textures and mineral compositions of meteorites are in good agreement with the postulated size of the potential source region for Martian meteorites during the impact of a small projectile (200 m), as defined by numerical modeling (Artemieva and Ivanov 2004). A comparison of shock pressures and ejection and terrestrial ages indicates that, on average, highly shocked fragments reach Earth-crossing orbits faster than weakly shocked fragments. If climatic changes on Mars have a significant influence on the atmospheric pressure, they could account for the increase of recorded ejection events of Martian meteorites in the last 5 Ma.

INTRODUCTION

More than 20 years ago, the hypothesis of a Martian origin for nine achondrites with unusually young crystallization ages was suggested (Wasson and Wetherill 1979; Walker et al. 1979; Nyquist et al. 1979; McSween and Stolper 1980; Wood and Ashwal 1981). This hypothesis is now widely accepted (Nyquist et al. 2001). A comprehensive compilation of the numerous publications concerning the Martian meteorites, edited by Meyer (2004), reflects the strong progress made in understanding the mineralogy and geochemistry of these rocks. The suite of Martian meteorites now consists of 51 fragments of 32 unpaired meteorites, with a total weight of approximately 89 kg (Fig. 1). These Martian meteorites document an interplanetary exchange of solid matter, which raises questions regarding the mechanism and the physical conditions during the ejection events. Especially the pressure/temperature (p/T) conditions have strong implications for the launching of Martian surface rocks (Artemieva and Ivanov 2002, 2004), for the retention of remanent magnetization (Weiss et al. 2000), the noble gas content (e.g., Schwenzer et. al. 2004), and a possible transfer of viable micro-organisms from Mars to Earth (Horneck et al. 2001).

To accelerate Martian rocks above the escape velocity (~5 km/sec; Wetherill 1984), various impact scenarios have been proposed, such as acceleration of the materials at a near-tangential impact incidence—ricochet (Swift and Clark 1983; Nyquist 1982); acceleration by shock vaporized buried ice (Wasson and Wetherill 1979; Wood and Ashwal 1981; O'Keefe and Ahrens 1983); turbulent mixing with material shocked to higher stresses (Swift and Clark 1983); or by high-density impact vapor plumes (O'Keefe and Ahrens 1986). Melosh (1984) proposed that the solid material is accelerated in a spallation zone, where the pressure gradient, but not the absolute shock pressure, is extremely high. Vickery and Melosh (1987) applied this model to a large-scale impact scenario with the ejection of 15 meter-size blocks that were later disrupted into meteorites in space. This scenario demands a crater size of no less than 200 km.

However, based on geochemical data and cosmic ray exposure (CRE) ages, four to eight different ejection events

© The Meteoritical Society, 2005. Printed in USA.

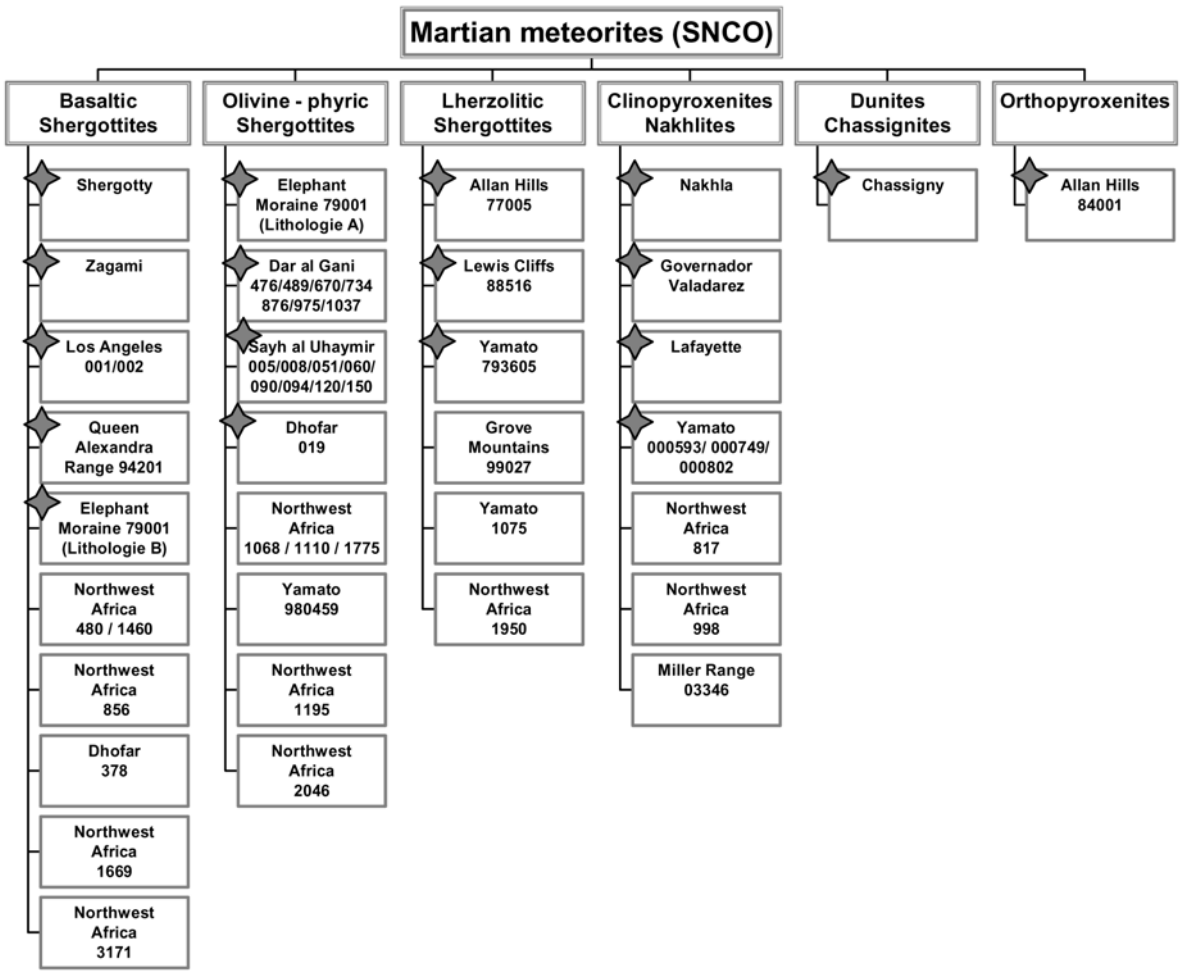

Fig. 1. The suite of Martian meteorites consists of 51 fragments of 32 unpaired meteorites, with a total weight of approximately 89 kg. The two lithologies A and B of EET 79001 are listed separately. The 17 unpaired Martian meteorites investigated in this study are indicated by stars. Compiled from Meyer (2004).

are documented by the suite of Martian meteorites (e.g., Nyquist et al. 2001), pointing to a different scenario with few moderate-magnitude impacts and the ejection of rather small, tens of centimeter-size fragments. Not considering atmospheric deceleration, Head at al. (2002) found that centimeter-size fragments can be ejected from Mars in vertical impacts forming craters as small as ~3 km in diameter. Neglecting atmospheric deceleration may, however, not be correct for the "small" impact scenario and centimeter-size fragments, as even such small particles can be decelerated in the low-density Martian atmosphere. On the other hand, in the more likely event of an oblique impact, the probable amount of Martian meteorites produced is substantially larger than expected from a vertical impact (Pierazzo and Melosh 2000; Artemieva and Shuvalov 2001).

In a recent study by Artemieva and Ivanov (2004), oblique impacts were simulated with a 3-D version of the SOVA code (Shuvalov 1999) coupled to ANEOS-derived (Thompson and Lauson 1972) equation of state (EOS) tables for the materials used. These authors modeled the oblique impacts of asteroids into both a dry (pure granite or basalt EOS) and wet (mixed granite/water EOS) Martian surface. These numerical simulations of oblique impacts on Mars indicate that spallation is indeed the only effective mechanism for the ejection of Martian meteorites. The size of the source region for potential Martian meteorites is laterally restricted to an area between 1 and 3 times the radius of the projectile (R) and extends to a depth of 0.2 R. The models show that, on average, the ejection velocity is positively correlated with shock pressure and negatively with distance to the impact center and burial depth of the ejected fragments. To be accelerated above the escape velocity, all escaping fragments had to be subjected to shock pressures in excess of ~10 GPa.

The energy to accelerate Martian surface rocks above the escape velocity is governed by shock waves. The process of shock compression and decompression causes significant shock effects in the shocked material, ranging from brittle and ductile deformation to melting or even vaporization.

Additionally, shock metamorphism could also lead to the transformation of minerals into their high-pressure polymorphs (e.g., Chao et al. 1960; Stöffler and Langenhorst 1994; Sharp et al. 1999; Langenhorst and Poirier 2000; Beck et al. 2004). To determine the shock pressures that affected the rocks, different pressure calibrations have been established (e.g., Dodd and Jarosewich 1979; Stöffler et al. 1991). The calibrations showed that, in the pressure range of 14 to 45 GPa, the shock-induced reduction of the refractive index of plagioclase is a reliable parameter to determine the recorded shock pressure (Stöffler et al. 1986). The different stages of progressive shock metamorphism of plagioclase range from diaplectic plagioclase (birefringent, shocked plagioclase) and diaplectic glass (maskelynite) to normal (thermal) glass, and were first described systematically in the Nördlinger Ries impact crater by Engelhardt et al. (1967) and Stöffler (1967). Maskelynite, the isotropic form (diaplectic glass) of plagioclase, which shows a conspicuous lack of flow features and vesiculation, was first discovered in the Shergotty meteorite by Tschermak (1872). Milton and DeCarli (1963) demonstrated that this material was formed by shock, and maskelynite has since been found in numerous shocked terrestrial, lunar, Martian, and meteoritic rocks (e.g., Bischoff and Stöffler 1992; Nyquist et al. 2001). Detailed investigations of naturally and experimentally shocked plagioclase showed that the refractive index of maskelynite systematically decreases with increasing shock pressure (Dworak 1969; Gibbons and Ahrens 1977; Stöffler and Hornemann 1972; Stöffler 1974; Ostertag 1983). Thus, based on the experimentally calibrated refractive index of maskelynite, the recorded shock pressure of the host meteorite can be deduced (Stöffler et al. 1986).

The mechanism and the physical conditions during the ejection events of Martian surface rocks investigated theoretically by numerical simulations (Head et al. 2002; Artemieva and Ivanov 2004) can only be evaluated by studying the physical conditions of the ejected material, which is represented by the suite of Martian meteorites. Numerical simulations and observations on Martian meteorites can, therefore, be combined to gain deeper insight in the transfer process of solid matter from Mars to Earth.

ANALYTICAL PROCEDURES

In this study, we investigated samples of 17 unpaired Martian meteorites (Fig. 1). We studied petrography and shock effects by transmitted and reflected light microscopy on thin sections of 16 Martian meteorites; only single plagioclase grains were available from Dhofar (Dho) 019. After optical inspection, the thin sections were investigated by a JEOL JSM-6300 scanning electron microscope (SEM) and backscattered electron images were taken of the meteorites' textures. Quantitative mineral analyses were obtained with a JEOL JXA-8800L electron microprobe operating at 15 kV and a beam current of 15 and 10 nA, respectively. To minimize the loss of volatile elements while analyzing plagioclase phases, Na and K were determined first in the measuring sequence and the beam size was defocused to 3–10 μm. Suitable mineral standards, including anorthoclase, basaltic glass, chromite, chromium augite, diopside, ilmenite, microcline, and plagioclase, all certified by the United States National Museum as reference samples for electron microprobe analysis (Jarosewich et al. 1980, 1987), were applied.

To determine the refractive indices of plagioclase phases, mineral separates from 15 meteorites were produced by crushing several milligrams of each meteorite in an agate mortar; the plagioclase grains from Dhofar 019 were kindly provided by G. Dreibus (Max-Planck-Institut für Chemie, Mainz), and for Yamato (Y-) 793605 only thin sections were studied. All plagioclase phases, ranging in size from 20 to 300 μm, were then hand-picked under a binocular. The immersion method was applied to determine the refractive index of the plagioclase phases (e.g., Kleber 1970). For this purpose, a heating stage was developed, which allows the plagioclase phases to be observed under the optical microscope while the stage temperature is adjusted in the range of 20 to 30 °C, with an accuracy of ±0.1 °C (Fritz et al. 2002). The plagioclase/maskelynite grains were embedded in different index liquids and the temperature was modified until the refractive index of the plagioclase phases was equal to that of the immersion liquid. A drop of the same liquid was placed in an Abbé refractometer. The temperature of the index liquid in the Abbé refractometer and of the index liquid containing the plagioclase/maskelynite grain was electronically controlled to be equal; the refractive index was then read from the Abbé refractometer with an accuracy of ±0.0004. The refractive index was measured at different edges of each grain. After these measurements, the grains were embedded in epoxy and prepared for further petrographic studies. The chemical composition was quantitatively determined by electron microprobe analysis in the same region of the grain where the refractive index had been measured. Finally, the refractive index data and chemical compositions of the plagioclase phases were plotted into a calibration diagram that allowed to deduce the shock pressures recorded by these plagioclase phases (Stöffler et al. 1986).

RESULTS

Shock Metamorphism

Determination of Shock Pressure

The results of the measurements on plagioclase phases are illustrated in Figs. 2 and 3, with the An content of the plagioclase phases plotted versus their refractive index. Generally in the diagrams, the three upper dotted lines represent the three main refractive indices of plagioclase

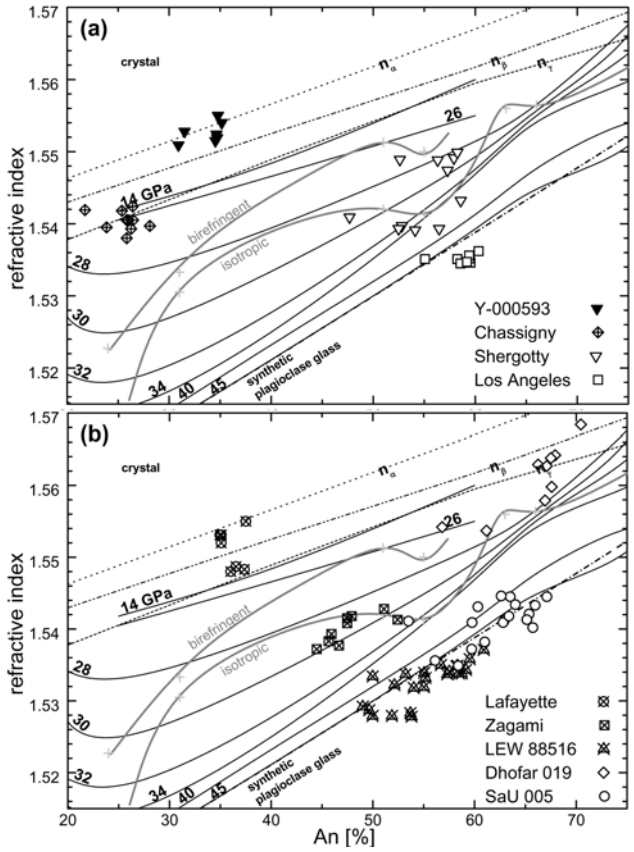

Fig. 2. Refractive indices of plagioclase phases and corresponding An contents for Y-000593, Chassigny, Shergotty, Los Angeles, Lafayette, Zagami, LEW 88516, Dhofar 019, and SaU 005. Refractive indices of plagioclase crystals and their isochemical glasses from Tröger (1982). Isobars and reference lines visualizing the optical properties of the diaplectic phases have been redrawn after Stöffler et al. (1986).

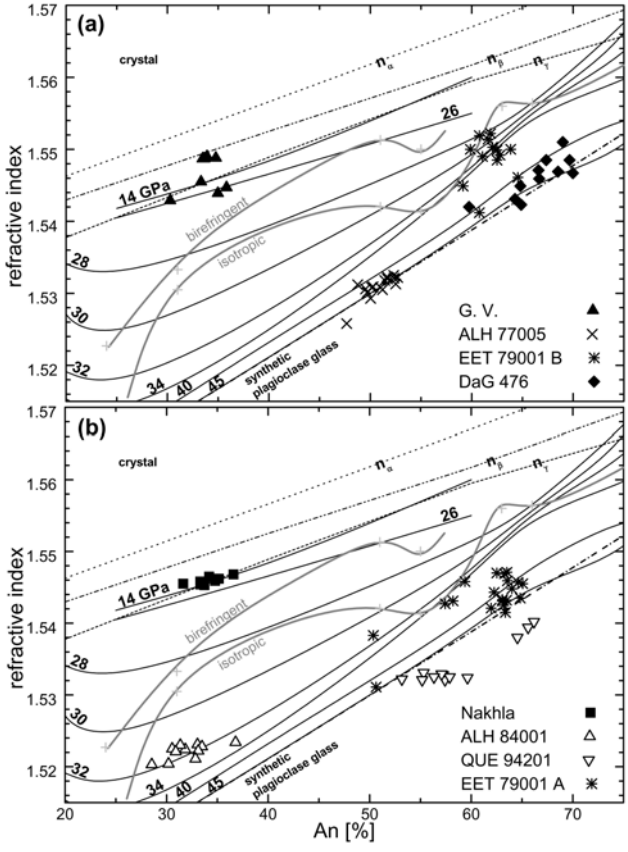

Fig. 3. Refractive indices of plagioclase phases and corresponding An contents for ALH 77005, DaG 476, Governador Valadares (G. V.), EET 79001 lithology A and B, ALH 84001, Nakhla, and QUE 94201. Refractive indices of plagioclase crystals and their isochemical glasses from Tröger (1982). Isobars and reference lines visualizing the optical properties of the diaplectic phases have been redrawn after Stöffler et al. (1986).

(n_α, n_β, n_γ), and the lower dotted line shows the refractive index of synthetic plagioclase glass. The pressure isobars represent the shock pressures needed to form diaplectic plagioclase or diaplectic glass of a certain chemical composition and refractive index. The gray lines visualize the optical properties of the diaplectic phases, ranging from birefringent to partly birefringent and totally isotropic.

Generally, all grains measured from the nakhlites, Chassigny, and the olivine-phyric shergottite Dhofar 019 were diaplectic plagioclase. Due to the unknown crystal orientation of these birefringent grains during the measurements, the lowest possible refractive index could not be determined unambiguously. The diaplectic plagioclase from Dhofar 019, however, showed only domains of very weak birefringence, and the crystallographic orientation should, thus, have had only minor influence on the refractive index measurements.

For the diaplectic plagioclase from Lafayette and Y-000593, the highest measured refractive indices correspond to the highest possible refractive index (n_α) of plagioclase, indicating that no shock-induced reduction of the refractive index occurred and, hence, the shock pressures were below 14 GPa (Figs. 2a and 2b). In contrast, all plagioclases from Nakhla and Governador Valadares exhibit refractive indices below n_β, with some grains having a refractive index below n_γ, corresponding to shock pressures in the range of 14 to 20 GPa (Figs. 3a and 3b). Birefringent diaplectic plagioclase from Chassigny clearly shows a shock-reduced refractive index (Fig. 2a). Combined with the petrographic observation of coexisting birefringent to partly birefringent (Fig. 4a) plagioclase and totally isotropic maskelynite, a shock pressure in the range of 26 to 32 GPa is inferred. Diaplectic plagioclase from Dhofar 019 displays a wide range of refractive indices, with the lowest index being close to the 28 GPa (Fig. 2b). Since total isotropisation, which was not observed in plagioclase from Dhofar 019, is achieved at shock pressures above 29 GPa (Stöffler et al. 1986), a shock pressure of 26 to 29 GPa is deduced for this meteorite.

The refractive indices of maskelynite from Shergotty and Zagami plot partly in the mixed regime of still partly

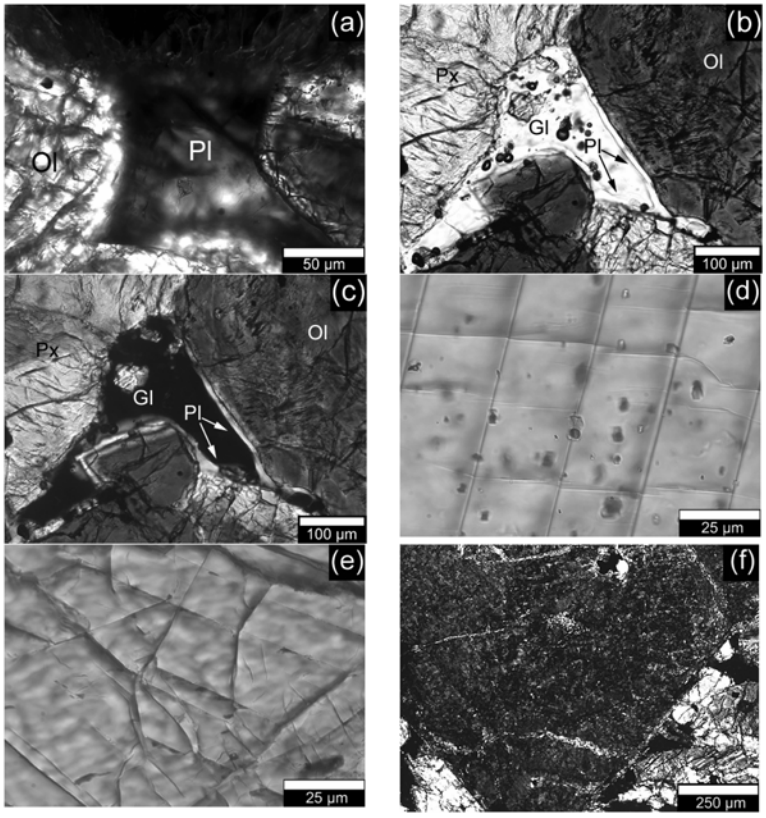

Fig. 4. Transmitted light images of a) birefringent diaplectic plagioclase in Chassigny (crossed polars); b–c) vesiculated plagioclase glass and birefringent plagioclase rim in ALH 77005. Note the unusual brown staining of olivine. b) Parallel polarizers. c) Crossed polarizers. d) Mechanical twinning in pyroxene of Y-000593 (crossed polarizers). e) Planar fractures in olivine from Nakhla (parallel polarizers). f) Strong mosaicism in olivine from SaU 005 (crossed polarizers). Ol = olivine; Pl = plagioclase; Px = pyroxene; Gl = glass.

birefringent to totally isotropic plagioclase, but mostly in the field of maskelynite (Fig. 2a and 2b). These results correspond to microscopic observations of very few weakly birefringent domains of diaplectic plagioclase in the maskelynite of these meteorites. Based on the average of all measurements, shock pressures of 30.5 ± 2.5 GPa for Shergotty and 29.5 ± 0.5 GPa for Zagami are determined.

In ALH 84001, no domains of weakly birefringent diaplectic plagioclase phases are present. All plagioclase phases represent maskelynite, with a high refractive index compared to an isochemical normal glass. The refractive indices of maskelynite from ALH 84001 attest to a shock pressure of 32 ± 1 GPa (Fig. 3b). Elephant Moraine (EET) 79001 is composed of at least two different lithologies, commonly referred to as an olivine-phyric lithology A and a basaltic lithology B (Fig. 1). Maskelynite from both lithologies plots into the field of diaplectic glass, with maskelynite of lithology A indicating slightly higher shock pressures than lithology B (Fig. 3a and 3b). This finding correlates with the larger amount of shock melt present in lithology A compared to lithology B. Shock pressures of 39 ± 4 GPa for lithology A and of 32 ± 3 GPa for lithology B are derived (the average of all data points from lithology A and B corresponds to a shock pressure of 36 ± 5 GPa). For Dar al Gani (DaG) 476 and Sayh al Uhaymir (SaU) 005 a shock pressure of 40 to 45 GPa is derived from measurements of the refractive indices for maskelynite (Figs. 2b and 3a).

Conspicuously, plagioclase phases in Lewis Cliff (LEW) 88516, Los Angeles, and Queen Alexandra Range (QUE) 94201 generally display significantly lower refractive indices than an isochemical synthetic plagioclase glass (Figs. 2a, 2b, and 3b). These differences cannot be explained by substantial loss of Na, as the electron microprobe analyses yielded stochiometric compositions for all grains measured, and the reason for this substantial lowering of refractive indices remains unclear. However, since the refractive indices of the plagioclase phases clearly deviate from those of thermal glass, these phases do not represent a quenched plagioclase melt but maskelynite, which limits the shock pressure to 45 GPa (Stöffler et al. 1986). As the calibration diagram of Stöffler et al. (1986) does not report refractive indices below the ones for synthetic glass, a shock pressure of 45 ± 3 GPa is deduced for maskelynite with the unusually low refractive indices in LEW 88516, Los Angeles, and QUE 94201.

ALH 77005 is the only sample of the suite investigated here, in which strongly vesiculated plagioclase melt is

common (Figs. 4b and 4c). This sample documents shock pressures in excess of the pressure range defined by the refractive index method applied here. In good agreement with this finding, the refractive index of the measured plagioclase glass is identical to that of synthetic plagioclase glass (Fig. 3a). A shock pressure higher than 45 GPa is needed to form the observed abundant shock melt of plagioclase (Stöffler and Hornemann 1972), indicating that ALH 77005 is the most highly shocked Martian meteorite in the current collection.

Shock Metamorphism of Olivine and Pyroxene

In addition to plagioclase, the main constituents of Martian meteorites are olivine and pyroxene, which also display shock effects (Figs. 4d–f, 5a, and 5b) that can be used to estimate the shock pressure (e.g., Stöffler et al. 1991; Bischoff and Stöffler 1992; Schmitt 2000). For the Martian meteorites studied here, the shock pressures obtained from shock effects in olivine and pyroxene are in excellent agreement with those deduced from the shock effects of plagioclase. In the nakhlites Lafayette and Y-000593, shock metamorphism is documented by mechanical twinning (Fig. 4d) and undulatory extinction in pyroxene and undulatory extinction in olivine, indicating a minimum shock pressure of 5 GPa (Stöffler et al. 1991). In the slightly higher shocked meteorites Nakhla and Governador Valadares, additional planar fractures in olivine are occasionally observed (Fig. 4e). With increasing shock pressure, a continuously increasing degree of undulatory extinction and a successive development of weak to strong mosaicism in olivine (Fig. 4f) and pyroxene are observed. In the meteorites subjected to shock pressures in excess of approximately 30 GPa, planar deformation features (PDFs) are developed in clinopyroxene (Fig. 5a) and planar micro-deformation in olivine (Fig. 5b) and orthopyroxene (we restrict the use of the term PDF to clinopyroxene, as olivine and orthopyroxene do not form diaplectic glass and, hence, do not form amorphous lamellae [Leroux 2001]). In the highly shocked ALH 77005, olivine additionally displays brown staining (Figs. 4b and 4c), which is produced by Fe oxidation at shock pressures above 44 to 56 GPa (Reimold and Stöffler 1978; Bauer 1979). Similar, although less intense, staining is found in LEW 88516.

To better constrain the maximum shock pressure in ALH 77005, the shock-induced effects on olivine and pyroxene can be used. Olivine in ALH 77005 lacks intergranular melting and intergranular recrystallization, which was observed in shock recovery experiments on dunite at shock pressures of 59 GPa (Reimold and Stöffler 1978). In addition, pyroxene does not show a significantly reduced birefringence, which according to Stöffler et al. (1991) starts to develop above ~50 GPa. Based on these observations an upper limit of the shock pressure of 55 GPa can be deduced for ALH 77005.

Localized Pressure and Temperature Excursions

Localized increases in pressure and temperature are a common phenomenon produced when a shock wave propagates through an inhomogeneous medium (e.g., Stöffler et al. 1991; Chen et al. 1996; Kenkmann et al. 2000; Heider and Kenkmann 2003). In Martian meteorites, the local shock pressure and temperature excursions produce localized brecciation, and with increasing shock pressures, melt veins and pockets.

In thin sections of the least shocked (5–14 GPa) nakhlites, Lafayette, and Y-000593, no brecciated or shock molten areas were observed, excluding significant p/T spikes. In contrast, very localized brecciated areas with a high fracture density are present in the slightly stronger shocked (14–20 GPa) nakhlites, Nakhla and Governador Valadares (Fig. 5c).

In Martian meteorites shocked above ~25 GPa, the formation of localized, 10 to several 100 μm wide, shock melt pockets is observed in Chassigny (Fig. 5d), Dhofar 019 (Badjukov et al. 2001), Shergotty, and Zagami. Additionally, melt veins are present in Zagami (Fig. 5e). In ALH 84001, no silicate melt was observed. However, this meteorite is a monomict breccia, consisting of large clasts, crosscut by granular bands of similar mineralogical composition (Fig. 5f). Carbonates had been deposited in cracks and in the granular bands. Maskelynite adjacent to the granular bands displays a sub-grain structure, with maskelynite fragments separated by a silica-rich glass (Fig. 6a). Some of these fragments show 120° grain boundaries, which probably formed during a late annealing event. Additionally, pyroxene fragments in the granular bands often fit together without intervening void spaces (Treiman 1998). Due to the deposition of pre-terrestrial carbonates in fractures of the granular zones, these deformation features were interpreted to have developed on Mars before the meteorites' ejection from that planet (Treiman 1998; Greenwood and McSween 2001).

In EET 79001, the two different lithologies, A and B, were subjected to different shock pressures according to the different refractive indices of maskelynite. In contrast to the less intensely shocked lithology B, which exhibits only minor shock melt, the more strongly shocked lithology A hosts complex-textured, relatively wide melt veins and pockets (Meyer 2004 and references therein; Fig. 6b). Melt pockets in EET 79001-lithology A range in width up to a few millimeters and consist of strongly vesiculated and weakly devitrified shock melt, occasionally hosting marginally melted remnants of either pyroxene or olivine.

In DaG 476, SaU 005, QUE 94201, and Los Angeles, all shocked above 40 GPa, melt pockets range in size from several 100 μm to several millimeters, and display complex recrystallization textures (Fig. 6c). Shock melt was quenched to glass, sometimes containing sizable vugs or abundant vesicles. In direct contact to the melt pockets, shock effects attesting to a high degree of shock metamorphism, i.e.,

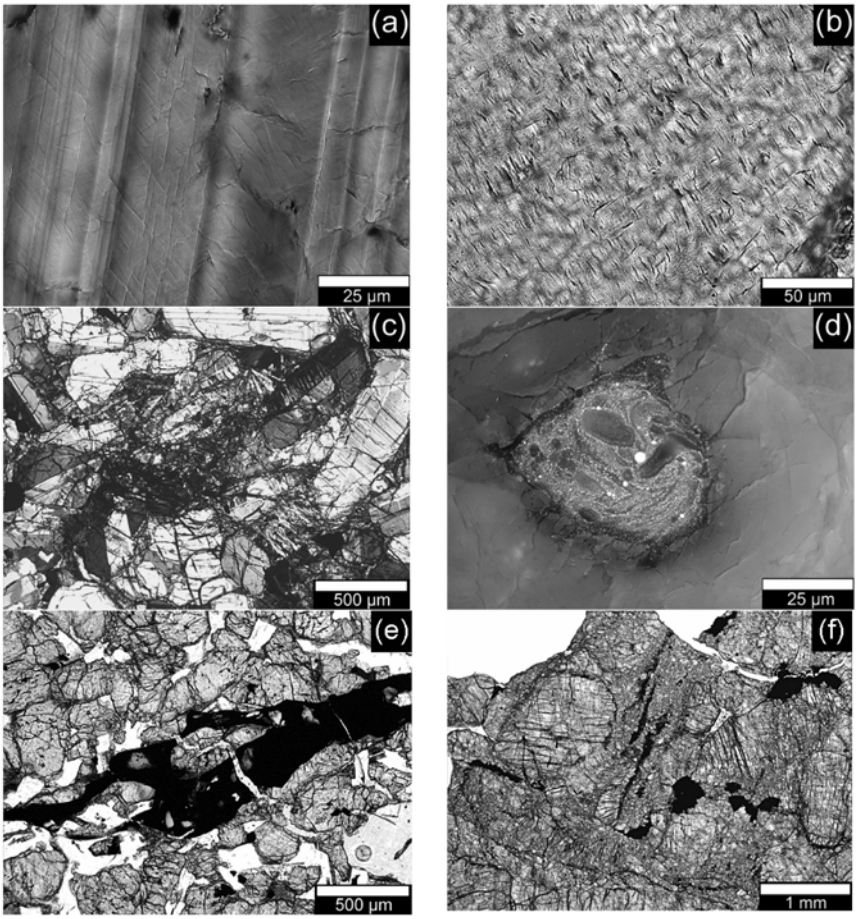

Fig. 5. Optical microscope images of a) planar deformation features in pyroxene of SaU 005, (crossed polarizers) and b) planar microdeformation in olivine in SaU 005 (parallel polarizers). c) A localized zone of high fracture density in Governador Valadares (crossed polarizers). d) A melt pocket in olivine of Chassigny with phosphate fragments and drops of opaque phases (reflected light). e) Melt vein in Zagami. f) Monomict brecciation in ALH 84001 (both with parallel polarizers).

staining in olivine, reduced birefringence of pyroxene, and partial melting of neighboring minerals, are observed.

In the lherzolitic shergottites ALH 77005 and LEW 88516, where the largest melt pockets are observed, small olivine and pyroxene crystals formed from the shock melt; grains adjacent to the melt pockets are recrystallized. Occasionally, off-shoots of now crystallized shock melt are seen injected into fractures of surrounding minerals (Fig. 6d). Due to the high post-shock temperature adjacent to these shock melt pockets, olivine and pyroxene are recrystallized. In the case of ALH 77005, which contains strongly Fe^{3+}-stained olivine, the recrystallized olivines often form bleached aureoles around the shock melt pockets. In Y-793605, only minor shock melting was observed. Except for ALH 84001, the lherzolitic shergottite Y-793605 is the only monomict breccia amongst the Martian meteorites. Granular zones crosscut thin melt veins (Fig. 6e) and some fragments of olivine, pyroxene, and plagioclase show flow textures (Fig. 6f), with the adjacent minerals being occasionally recrystallized.

Shock Temperature

Shock Heating of Meteorites

As a shock wave propagates through matter, a certain amount of energy is deposited as waste heat in the decompressed shocked material. The method to calculate the post-shock temperature for known Martian meteorites has been described in detail by Artemieva and Ivanov (2004). It is based on the experimental equation of state (EOS) (Stöffler 1982; Trunin et al. 2001) for terrestrial rocks with similar composition and a linear relation of the particle velocity U to shock wave velocity D: $D = c + sU$, with c and s experimentally determined constants (e.g., Melosh 1989).

The problem with this approach is that at high pressures (32 to 44 GPa for the experimentally shocked rocks used by Artemieva and Ivanov 2004) certain minerals in the shocked rocks undergo phase transitions. Therefore, the related c and s values change substantially and estimates that do not take this transition into account become inaccurate. Thus, to determine the shock temperatures corresponding to high shock

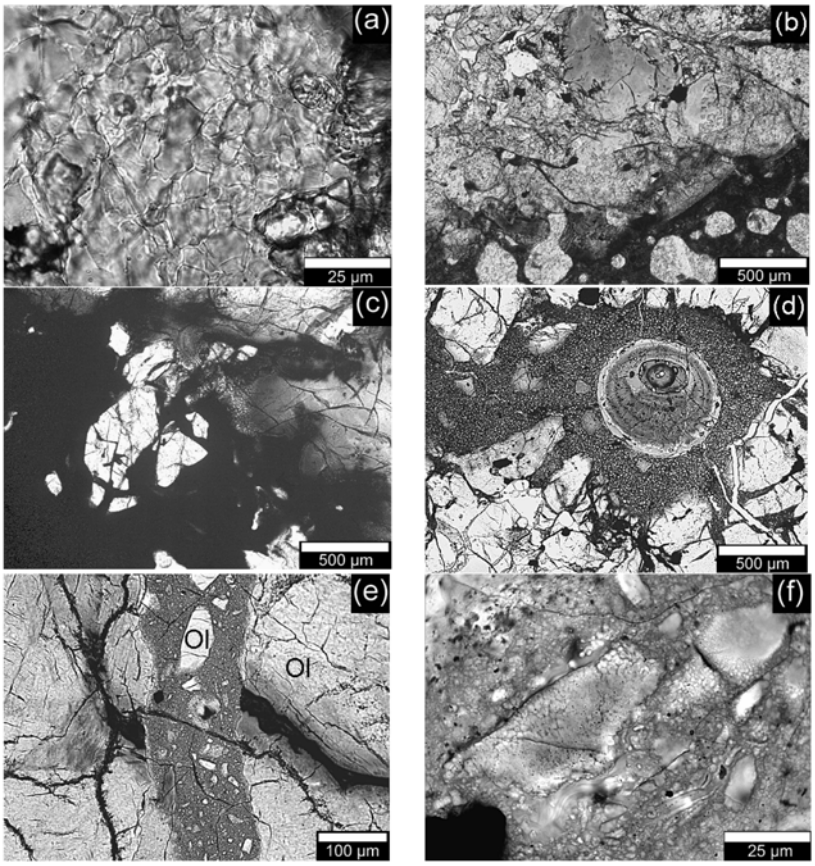

Fig. 6. Transmitted light images with parallel polarizers of a) sub-grain structure in maskelynite of ALH 84001 adjacent to granular band; b) devitrified melt pocket with large vugs in EET 79001-A; adjacent olivine and pyroxene are recrystallized and close to the melt pocket. One olivine crystal displays unusual brown staining. c) An opaque melt in QUE 94201 engulfing birefringent phosphate grains; shock blackening and recrystallization texture is developed in the adjacent pyroxene. d) A large shock melt pocket with complex texture from ALH 77005. e) A granular band in monomict breccia Y-793605 cutting through a melt vein. f) A granular band in Y-793605 illustrating the band's low porosity and the flow texture of some fragments. Ol = olivine.

pressures, a different approach was taken here. To determine the energy released (e_{Rl}, e_{Rh}) during decompression, we integrated along the two branches of the Hugoniot: from zero pressure (or zero particle velocity) to the pressure corresponding to the phase transition P_* (particle velocity U_*, shock velocity D_*, $D_* = c_l + s_l U_*$):

$$e_{Rl} = \frac{c_l}{s_l}\left[U_* - \frac{c_l}{s_l}\ln\left(1 + \frac{s_l}{c_l}U_*\right)\right] \quad (1)$$

and then from the phase transition pressure to the final pressure P_{max} (corresponding to the final particle velocity U_{max}, the shock velocity D_{max}):

$$e_{Rh} = \frac{c_h}{s_h}\left(U_{max} - U_* - \frac{c_h}{s_h}\ln\frac{c_h + s_h U_{max}}{c_h + s_h U_*}\right) \quad (2)$$

Finally, the post-shock temperature increase is $T = (e_H - e_{Rl} - e_{Rh})/C_p$, where e_H is $U^2/2$ and is the Hugoniot total energy. The specific heat capacity, C_p, differs from material to material and depends on the temperature. However, the value of 1000 J/kg/K is a reasonable approximation for the investigated mafic to ultramafic rocks (Waples and Waples 2004).

The calculated post-shock temperatures are presented in Table 1, and shock pressure has been plotted versus post-shock temperature in Fig. 7. Experimentally derived EOS for Stillwater pyroxenite, Twin Sister dunite (Stöffler 1982), and a gabbroic rock (Trunin 2001) were used to estimate the post-shock temperatures of the Martian meteorites (Table 1).

The nakhlites represent the least shocked Martian meteorites and were subjected to only minor post-shock temperature elevations of less than 30 °C. Calculations of the post-shock temperature in the range of 26 to 32 GPa yield a post-shock temperature elevation of 40 to 60 °C for Chassigny. For ALH 84001, shocked between 31 to 33 GPa, a post-shock temperature elevation of 100 to 110 °C was derived. In shergottites, the recorded shock pressures range from 20 to 55 GPa. At shock pressures in the range of 20 and 30 GPa, the post-shock temperature elevations vary between 50 and 100 °C, from 30 to 35 GPa they increase up to 200 °C, and at 45 GPa a post-shock temperature elevation of nearly

Table 1. Compilation of crystallization, ejection, and terrestrial ages as well as of shock metamorphic data of Martian meteorites.

Sub-group	Meteorite	Crystallization age (Ma)	Ejection age (Ma)	Terrestrial age (Ma)	Shock pressure (GPa) in		Post-shock temperature increase ΔT (K)	Reference rock
					This work	Literature		
Basaltic shergottite	Shergotty	165 ± 4[a]	3.0 ± 0.3[e]	Fall	30.5 ± 2.5	29 ± 1[p]	100 ± 50	Gabbro[v]
	Zagami	177 ± 3[a]	3.0 ± 0.3[e]	Fall	29.5 ± 0.5	29.3[q] 31 ± 2[p] 27[r]	70 ± 5	
	QUE 94201	327 ± 10[a]	2.8 ± 0.3[e]	0.29 ± 0.05[i]	45 ± 3		560 ± 120	
	Los Angeles	170 ± 8[a]	3.0 ± 0.3[e]		45 ± 3		560 ± 120	
	EET 79001 B				32 ± 3			
Lithology A + B	EET 79001	173 ± 3[a]	0.73 ± 0.15[a]	0.012 ± 0.002[j]	36 ± 5	34 ± 1r	240 ± 160	
Olivine-phyric shergottites	EET 79001 A				39 ± 4			
	DaG 476	474 ± 11[a]	1.25 ± 0.2[a]	0.060 ± 0.02[k]	40–45		470 ± 100	
	SaU 005		1.2 ± 0.3[e]		40–45	>45[s]	470 ± 100	
	Dhofar 019	575 ± 7[b]	19.8 ± 2.3[f]	0.34 ± 0.04[l]	26–29		60 ± 10	
	Y-980459	304 ± 82[c]	1.1 ± 0.2[g]			20–25[t]	50 ± 5	
Lherzolitic shergottites	ALH 77005	179 ± 5[a]	3.8 ± 0.7[e]	0.2 ± 0.07[m]	45–55	43 ± 2[p] 45[l]	800 ± 200	
	LEW 88516	178 ± 8[a]	3.9 ± 0.4[e]	0.021 ± 0.01[a]	45 ± 3		560 ± 120	
	Y-793605	212 ± 62[a]	4.7 ± 0.5[a]	0.035 ± 0.035[a]		40–45[u]	470 ± 100	
Nakhlites	Nakhla	1270 ± 10[a]	10.8 ± 0.8[e]	Fall	14–20		20 ± 10	Pyroxenite[w]
	Governador Valadares	1330 ± 10[a]	10.0 ± 2.1[a]	A few hundred yr[n]	14–20		20 ± 10	
	Lafayette	1320 ± 20[a]	11.9 ± 2.2[a]	0.0029 ± 0.0010[n]	5–14		10 ± 5	
	Y-000593	1300 ± 20[d]	12.1 ± 0.7[h]	0.055 ± 0.02[g]	5–14		10 ± 5	
Orthopyroxenite	ALH 84001	4510 ± 110[a]	14.7 ± 0.9[e]	0.0065 ± 0.001[o]	32 ± 1		105 ± 5	
Chassignites	Chassigny	1340 ± 50[a]	11.1 ± 1.6[e]	Fall	26–32		50 ± 10	Dunite[w]

[a]Nyquist et al. (2001); [b]Borg et al. (2001); [c]Shih et al. (2003); [d]Misawa et al. (2003); [e]Eugster et al. (2002); [f]Shukolyukov et al. (2000); [g]Nishiizumi and Hillegonds (2004); [h]Okazaki et al. (2003); [i]Nishiizumi and Caffee (1996); [j]Jull and Donahue (1988); [k]Nishiizumi et al. (2001); [l]Nishiizumi et al. (2002); [m]Nishiizumi et al. (1986); [n]Jull et al. (1999); [o]Jull et al. (1994); [p]Stöffler et al. (1986); [q]Langenhorst et al. (1991)' [r]Lambert (1985); [s]Gnos et al. (2002); [t]Greshake et al. (2004); [u]Fritz et al. (2005); EOS for temperature calculations from [v]Trunin et al. (2001); and [w]Stöffler (1982).

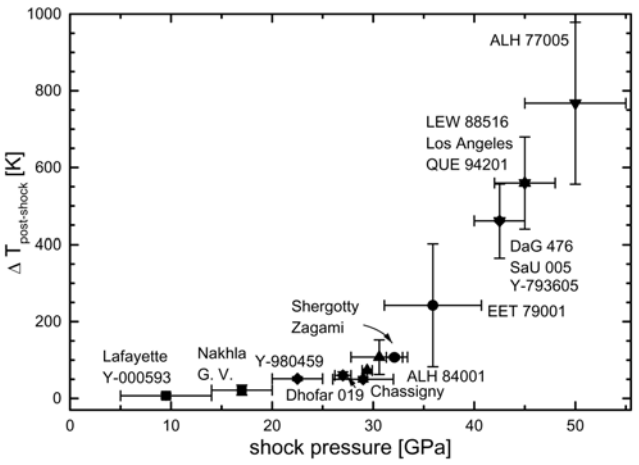

Fig 7. Post-shock temperature versus shock pressure of Martian meteorites. The post-shock temperature estimates are based on experimentally determined equations of state from mafic to ultramafic rocks (Stöffler 1982; Trunin et al. 2001). Corresponding data are given in Table 1. G. V. = Governador Valadares.

600 °C was determined. For a shock compression of 55 GPa, which is possibly recorded in the most highly shocked Martian meteorite, ALH 77005, a post-shock temperature increase of approximately 1000 °C is calculated.

Petrological and Physical Observations Regarding Post-Shock Temperature

Some petrological and physical characteristics of the Martian meteorites contain information concerning the post-shock temperature, allowing some comparison with the calculated temperatures. After passage of the shock wave, the initial temperature of the rocks (surface temperature on Mars) is increased by the post-shock temperature resulting in an absolute temperature for the meteorite after ejection. Weiss et al. (2000) studied the magnetic characteristics of ALH 84001 samples and found that: 1) these samples have a spatially heterogeneous pattern of magnetization, and 2) the samples lose their magnetization after heating to 40 °C and cooling in a zero magnetic field. This means that the rock was not heated above 40 °C since its ejection from the surface of Mars. As the calculated post-shock temperatures for ALH 84001 range between 100 and 110 °C, it can be assumed that the pre-impact temperature of the ALH 84001 parent rock was below –60° to –70 °C. This assumption seems reasonable, as temperatures on the surface of Mars vary between –130° and +20 °C (Lodders and Fegley 1998).

For the most strongly shocked Martian meteorite, ALH 77005, the high post-shock temperature is documented by the recrystallization of plagioclase. Annealing experiments of maskelynite show that labradorite shocked to 45 GPa requires 0.5 hr at 1000 °C or 10 hr at 900 °C to display signs of recrystallization (Ostertag 1982). At 1000 °C for 1 hr and 50 hr at 900 °C almost all plagioclase could be recrystallized in the annealing experiments (Ostertag 1982). The recrystallized rim of birefringent plagioclase in ALH 77005 documents that elevated temperatures in the meteorite prevailed long enough to initiate recrystallization, but not long enough to allow complete recrystallization, of plagioclase. For shock compression between 45 and 55 GPa, the calculated post-shock temperatures range from 600° to 1000 °C. Thus, the observed recrystallization of plagioclase is in good agreement with the upper limit of the deduced shock pressure at 55 GPa for ALH 77005.

Cooling Time for Meteorites in Space

After ejection from Mars, the rocks cooled from the shock-heated temperature to an ambient temperature in space. To estimate the cooling time of Martian meteorites in space, the heat transfer in a sphere with radius, *R*, was numerically solved by:

$$\frac{\partial e}{\partial t} = \frac{1}{r^2}\frac{\partial}{\partial r}\left(kr^2\frac{\partial T}{\partial r}\right),\ T(r,t=0) = T_{ps}, T(r=R,t) = 0. \quad (3)$$

$$e = \rho C_p T \quad (4)$$

The initial (at time $t = 0$) constant temperature T_{ps} is equal to a post-shock temperature estimated from the value of the maximum shock compression. The material properties, density ρ, heat capacity C_p, and the thermal conductivity k, depend on the temperature. Because temperature changes with time, these values depend on the size of the body (r).

The real density of ALH 77005 was estimated to be 2830–2890 kg/m^3 (McSween 2002). Data compilations for the heat capacity of the rocks and their temperature dependence from Lu et al. (1994) and Waples and Waples (2004) give a C_p = 1000–1300 J/kg/K in the temperature interval of 300–1000 K, with a roughly linear increase of $C_p(T)$. The thermal conductivity for mantle rocks is 5–3 W/m/K, for the same temperature range (Hofmeister 1999). A linear decrease of k with temperature was used, although the real dependence is more complex. Finally, the thermal diffusivity increases from 0.7 mm^2/sec at 1000 K to 1.7 mm^2/sec at 300 K. The equations were solved numerically by using an implicit finite difference scheme and centering the values of heat capacity and thermal conductivity appropriately. Additional iterations on each time step may be performed. However, the calculations showed that they do not change the results substantially.

Figure 8 shows the temperature development in the center of a sphere of an ultramafic rock 1 m in diameter and heated by shock to 1000 and 900 °C. It can be seen that the temperature is practically constant for 3 hr and then drops rather quickly at a rate of about 50 °C/hr. Internal properties of the heat-transfer equations allow the recalculation of these curves for any arbitrary size. The results show that a sphere at least 0.44 m in diameter is needed to keep the temperature for 0.5 hr at 1000 °C to initiate recrystallization of plagioclase.

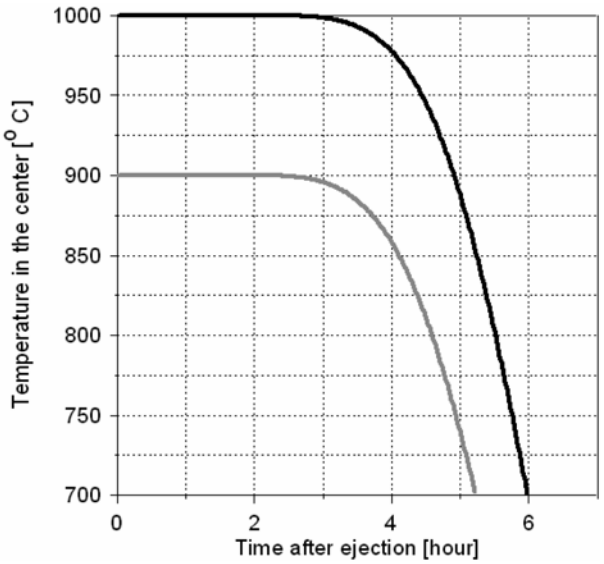

Fig. 8. Cooling in space of a sphere of ultramafic rock 1 m in diameter shock-heated to 1000 °C (black line) and 900 °C (gray line), respectively.

For complete recrystallization, the sample must be at the same temperature twice as long, i.e., its size should be 1.4 times larger. This size, 0.4–0.6 m, is in good agreement with the size of the largest fragments obtained by numerical modeling (0.24–0.75 m; Artemieva and Ivanov 2004) and with measurements of epithermal neutron fluxes, indicating that the minimum pre-atmospheric radii of the investigated Martian meteorites were in the range of 0.22–0.25 m (Eugster et al. 2002). If the initial temperature of the ejected fragment was lower than, e.g., ~900 °C, then its size should be larger than 1.9 m. This rather large size is, however, not in agreement with the small, ~3 km in diameter crater scenario (Head et al. 2002; Artemieva and Ivanov 2004), although larger impacts certainly could produce such fragments and enable them to escape Mars.

DISCUSSION

Shock Pressures

A comparison of the determined shock pressures with literature data, which are based also on the shock-induced reduction of the refractive index of plagioclase, confirms the reliability of the applied method (Table 1). Generally, similar results were obtained from different samples of the same meteorite proving that the measurements of the refractive indices yield reproducible data throughout the entire meteorite. The shock pressures derived from the reduction of the refractive index of plagioclase and the textures of melt pockets differ substantially in the two EET 79001 lithologies A and B. This difference could possibly indicate a higher porosity of lithology A compared to lithology B, as the closure of gaps and voids induces a second shock wave superposing and amplifying the primary wave (Heider and Kenkmann 2003).

In addition to the properties of minerals and rock texture, the noble gas content of meteorites is significantly influenced by shock events, leading to an almost complete loss of He at shock compression in excess of about 35 GPa (Stöffler et al. 1991). A comparison of the loss of He in the Martian meteorites investigated in the present study with respect to the determined shock pressures displays a strong correlation for eight meteorites shocked below 40 GPa, with the most highly shocked meteorites showing the highest loss of He; the four Martian meteorites shocked above 40 GPa show a complete loss of He (Schwenzer et al. 2004). It should be noted that He loss was observed in all 12 investigated Martian meteorites, including the very weakly shocked nakhlite Lafayette (Schwenzer 2004; Schwenzer et al. 2004). In ordinary chondrites no loss of noble gases was detected at shock pressures below 10 GPa (Stöffler et al. 1991), and so the Martian meteorites should have experienced shock pressures of at least 10 GPa.

In summary, it can be concluded that the estimated shock pressures based on the progressive shock metamorphism of plagioclase are in excellent agreement with various other shock metamorphic features in Martian meteorites.

P/T Launch Conditions

Knowledge of the degree of shock metamorphism observed in Martian meteorites allows to constrain the p/T launch conditions for Martian surface rocks. Shock features in rock-forming minerals of Martian meteorites, Raman spectra of plagioclase phases (Fritz et al. 2004, 2005), and He loss in Martian meteorites (Schwenzer et al. 2004) show that all Martian meteorites investigated in the present study display signs of shock metamorphism of at least 5 to 14 GPa. Petrographic descriptions of the 15 meteorites not investigated in this study allow to extend this conclusion over the entire suite of Martian meteorites (Table 2)(Meyer 2004). In all shergottites that were not investigated here, plagioclase was transformed to maskelynite, with the exception of Dhofar 378, which contains vesiculated plagioclase glass and recrystallized plagioclase (Mikouchi and McKay 2003), indicating that all these meteorites experienced shock pressures in the range of 30 to 45 GPa. The lherzolitic shergottite Y-793605 was subjected to shock pressures of 40 to 45 GPa (Fritz et al. 2005), and the olivine-phyric shergottite Y-980459, which does not contain plagioclase phases, has been reported to be shocked between 20 and 25 GPa (Greshake et al. 2004). The three known nakhlites, which were not investigated here, have been described to be mildly (below ~25 GPa) shocked (Meyer 2004 and references therein).

The observation that all known Martian meteorites display degrees of shock metamorphism of at least 5 to 14 GPa strongly supports the prediction from numerical

Table 2. State of plagioclase phases in all known Martian meteorites based on observations and literature data (Meyer 2004).

Sub-group	Total no.	No plagioclase	Diaplectic plagioclase	Maskelynite	Vesiculated glass	Recrystallized plagioclase
Nakhlites	7	1	6	–	–	–
Chassigny	1	–	1	1	–	–
ALH 84001	1	–	–	1	–	–
Basaltic shergottites	10	–	2	9	1	1
Olivine-phyric shergottites	8	1	1	8	–	–
Lherzolitic shergottites	6	–	–	6	1	1

modeling that no material can be ejected from the surface of Mars without experiencing a shock pressure of at least 10 GPa (Artemieva and Ivanov 2004).

Sampling Depth

Numerical models of oblique impacts on Mars show that the size of the Martian meteorite source region is laterally restricted to 1 to 3 times the radius of the projectile (R) and extends to a depth of 0.2 R (Fig. 9) (Artemieva and Ivanov 2004). These theoretical predictions can be tested by evaluating the pre-impact position of the meteorites' parent rocks. For this, the sampling depth of a 200 m projectile (equal to 0.2 R of the projectile) and the burial depth of the source rocks of the Martian meteorites are shown in Fig. 10.

A minimum depth of the parent rocks is defined by the meteorites' cosmic ray exposure (CRE) ages. The lack of 2–π CRE ages for most Martian meteorites indicates that their original position was at a depth of at least 1 m (Warren 1994). The only Martian meteorites that were possibly exposed to cosmic rays on the parent body are the monomict breccia Y-793605 (Nagao et al. 1997) and Y-980459 (Nishiizumi and Hillegonds 2004).

More precise information on the burial depth can be obtained from the texture, the composition of minerals, and, for example, from the microstructures in the pyroxene of these meteorites. From these petrologic data, the maximum burial depth for final solidification in either a magma chamber or a lava flow can be inferred. For nakhlites and possibly Chassigny (Monkawa et al. 2004), as well as for the basaltic and olivine-phyric shergottites, the final solidification in a near-surface position corresponds to the size of the Martian meteorite source region of a small projectile (Fig. 10). Petrologic characteristics of ALH 84001 and the lherzolitic shergottites possibly indicate a deeper burial depth. This may imply a larger impact. Alternatively, the parent rocks could have been either exposed by erosion or exhumed and transferred to the source region by volcanism or impact cratering. Only two Martian meteorites, ALH 84001 and the lherzolitic shergottite Y-793605, are monomict breccias. These textures developed after crystallization of the rocks, and for ALH 84001, several petrologic characteristics indicate that the brecciation developed on Mars before the ejection event (Treiman 1998). These textural characteristics, i.e., monomict brecciation and transecting melt veins and granular bands, of ALH 84001 and Y-793605 may suggest a multi-stage impact history.

Transfer Time

Modeling of the orbital evolution of ejected fragments, and radionuclide data for Martian meteorites indicate orbital differences of these fragments, because those reaching Earth-crossing orbits faster have a lower entrance velocity into the Earth's atmosphere compared to those meteorites that take more time to be transferred to Earth (Garrison et al. 1995; Swindle et al. 1996; Gladman 1997). By modeling the orbital evolution of small bodies ejected from Mars, the remnant velocity at the time when the particles have effectively escaped the Martian gravitational field was found to be an important parameter for the delivery efficiency and travel time (Wetherill 1984; Gladman 1997). Fragments with high remnant velocity reach Earth-crossing orbits faster than fragments with lower remnant velocity (Gladman 1997). Numerical simulations of impacts also show that the ejection velocity is positively correlated with the shock pressure (Artemieva and Ivanov 2004). This means that, on average, the most highly shocked fragments were ejected with the highest ejection velocity, thus retaining the highest remnant velocity and on average reaching Earth-crossing orbits in the shortest time.

This assumption can now be verified by comparing shock pressure and transfer time of Martian meteorites. On average, Martian meteorites with young ejection ages were subjected to higher shock pressures compared to the ones with older ejection ages, and none of the Martian meteorites with old ejection ages (>5 Ma) experienced a shock pressure in excess of 35 GPa (Figs. 11a and b). The young shergottites with ejection ages of less than 5 Ma generally experienced high shock compression (>25–30 GPa). The only exception is Y-980459, which experienced a shock compression of only 20 to 25 GPa (Greshake et al. 2004). For Y-980459, the high cooling rates (Greshake et al. 2004) and a 2–π CRE geometry (Nishiizumi and Hillegonds 2004) indicate a pre-impact depth position of less than 1 m. As for a given shock pressure, the ejection velocity decreases with burial depth (Artemieva

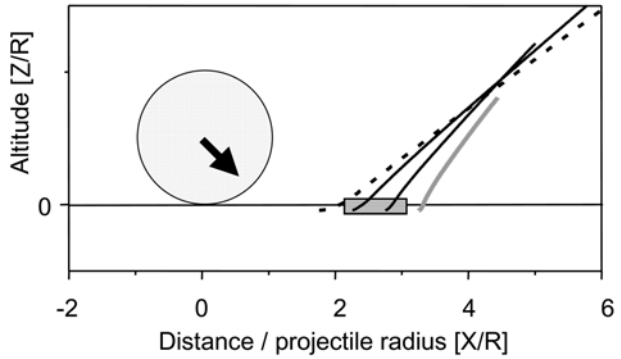

Fig. 9. The Martian meteorite ejection process: a spherical projectile strikes the surface at 45 degrees with a velocity of 10 km/sec. The high-velocity ejecta from closest to the impact point are molten (dashed line), the ones originating from an area most distal to the point of impact are solid but characterized by velocities lower than escape velocity (gray line). In between lies the source region of the Martian meteorites (solid lines), marked by a rectangle. Modified after Artemieva and Ivanov (2004).

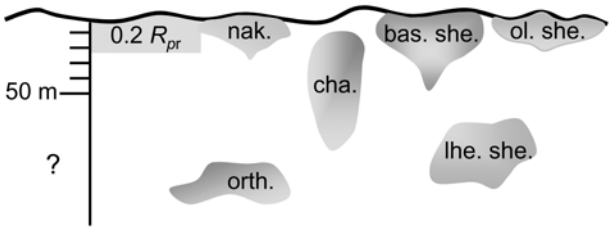

Fig. 10. Sampling depth of a 200 m projectile (0.2 R) and depth for final magmatic solidification of the source rocks of basaltic shergottites (bas. she.), olivine-phyric shergottites (ol. she.), lherzolitic shergottties (lher she.), nakhlites (nak.), Chassigny (cha.), and the orthopyroxenite ALH 84001 (orth.), as infered from their petrological characteristics (e.g., McCoy et al. 1992; Müller 1993; McCoy and Lofgren 1999; Mikouchi et al. 2001; Mikouchi and Miyamoto 2002; Koizumi et al. 2002; Taylor et al. 2002; Mikouchi et al. 2003; Szymanski et al. 2003; Greshake et al. 2004; Monkawa et al. 2004). See text for details.

and Ivanov 2004), a shallow pre-impact position could have allowed Y-980459 to be ejected at high velocities, while the rock experienced a relatively low shock pressure. The shergottite Dhofar 019, ALH 84001, Chassigny and especially the nakhlites were generally affected by lower shock compression in the ejection event and appear to have been stored in heliocentric orbits for longer times.

The orbital parameters of Mars, at the time of the impact and with regard to the direction of ejection relative to the apex of Mars, influence the orbital evolution of the particles. To minimize these uncertainties, we restricted the comparison of Martian meteorites to those that originated from the same ejection event and compared their terrestrial residence time with shock pressures. By comparing the terrestrial ages of Martian meteorites from the same ejection event, it can be determined which meteorite had the fastest transit from Mars to Earth.

Two different ejection events are compared in Fig. 11b. The first event is represented by the lherzolitic shergottites, ALH 77005, LEW 88516, and Y-793605. These meteorites display striking petrological similarities, which indicate that they could originate from the same igneous complex (Mikouchi and Miyamoto 2000). Their ejection ages group around 4 Ma, but have some significant differences (3.8–4.7 Ma; Nyquist et al. 2001; Eugster et al. 2002). Y-793605 yields a higher CRE age than ALH 77005 and LEW 88516, which could result from irradiation by cosmic rays at the surface of Mars (Nagao et al. 1997). Compared to the relatively long terrestrial residence time of 200 ± 70 ka for the most highly shocked Martian meteorite ALH 77005 (45–55 GPa), the two less shocked lherzolitic shergottites LEW 88516 (45 ± 3 GPa; 21 ± 10 ka) and Y-793605 (40–45 GPa; 35 ± 35 ka) are reported to have a shorter terrestrial residence time (Fig. 11b; Table 1) and, hence, needed more time to be transfered to Earth.

For the second event, represented by Shergotty (30.5 ± 2.5 GPa), Zagami (29.5 ± 0.5 GPa), Los Angeles, and QUE 94201 (both 45 ± 3 GPa), the ejection ages group around 3 Ma and are indistinguishable within analytical error (Nyquist et al. 2001; Eugster et al. 2002). The terrestrial ages for Zagami and Shergotty are low as these meteorites represent observed falls, and QUE 94201 resided in Antarctica for 290 ± 50 ka (Nishiizumi and Caffee 1996). Unfortunately, the terrestrial age of the Los Angeles meteorite is not known.

Concerning the two events described above, namely the basaltic (~3 Ma) and lherzolitic (~4 Ma) shergottite ejection events, the most highly shocked meteorites (QUE 94201 and ALH 77005, respectively) reached Earth first.

The nakhlites and Chassigny that were all subjected to shock pressures below 32 GPa most probably originate from the same ejection event before ~11 Ma (Table 1). This third event, involving samples for which shock pressures and terrestrial ages are available, is not shown in Fig. 11b because these meteorites all have short terrestrial ages. The nakhlites and Chassigny are either observed falls or resided on Earth for less than 5 ka (Jull et al. 1999), with the exception of Y-000593, which exhibits a slightly higher terrestrial age of 50 ± 20 ka (Nishiizumi and Hillegonds 2004). Compared to their long transfer time of 11 Ma, these moderately to weakly shocked (<32 GPa) meteorites arrived on Earth at similar times.

In summary, our shock barometric data, in combination with radionuclide data on Martian meteorites, indicate a correlation between short transfer time and high shock pressure. Furthermore, the assumption that the degree of shock pressure influences the transfer time of Martian meteorites to Earth could also explain the lack of highly shocked (>35 GPa) meteorites from ejection events older than 5 Ma. In Antarctica, an area that has some of the best preservation conditions for all types of meteorites on the surface of Earth, the terrestrial ages of all but a few of these

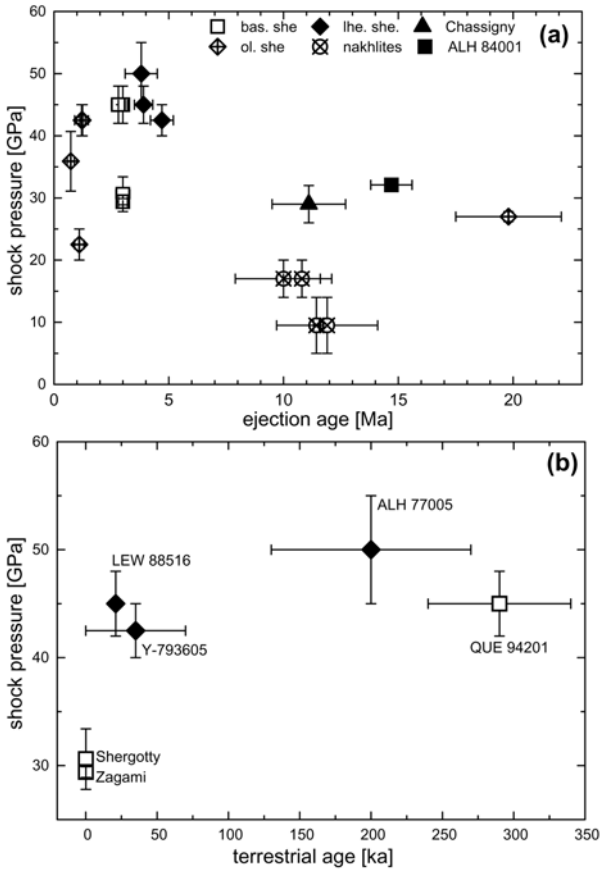

Fig. 11. a) Ejection age versus shock pressure. b) Terrestrial age versus shock pressure. Data of ejection and terrestrial ages are listed in Table 1 (bas. she. = basaltic shergottites; ol. she. = olivine-phyric shergottites; lhe. she. = lherzolitic shergottites).

meteorites are less than 1 Ma (Welten et al 1997; Welten et al. 1999). Given the limited preservation of meteorites on Earth, the lack of highly shocked nakhlites may be due to the fact that they were transferred to Earth substantially faster than the weakly shocked ones, and, therefore, are less likely to be preserved over a given time.

Influence of Atmospheric Density Variations

The cosmic ray exposure ages of Martian meteorites are unevenly distributed in time and can be grouped into four to eight different ejection events (Fig. 12) (Nyquist et al. 2001; Eugster et al. 2002). In the last 5 Ma, one to four ejection events sampled source regions younger than 1 Ga, and in the preceding 5 to 20 Ma three to four different ejection events sampled source regions ranging in age between 0.1 and 4.5 Ga, as recorded by the Martian meteorites (Fig. 12; Table 1). As the climate on Mars, and possibly the atmospheric pressure, have not been constant in the last 20 Ma (Ward 1974; Barker 2001; Mustard et al. 2001; Laskar et al. 2002; Head et al. 2003), we have evaluated a possible influence of climatic variations on the production rate of Martian meteorites.

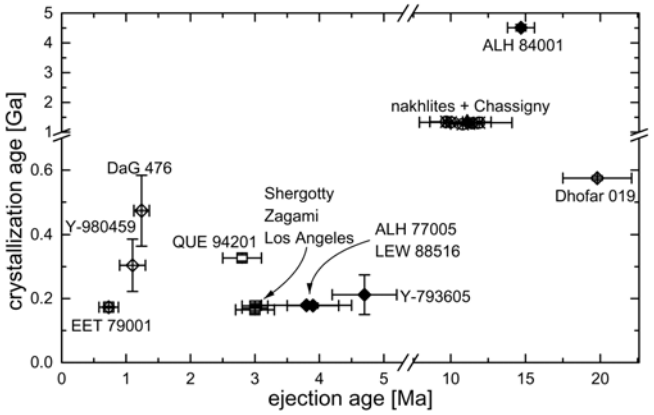

Fig. 12. Ejection age versus crystallization age of Martian meteorites. Data of ejection and crystallization ages are given in Table 1.

The minimum size of a fragment that retains a velocity above the escape velocity in the post-impact plume depends on the scale of the impact event and on the density of the atmosphere. Even tiny particles escape in a very large impact or on planetary bodies without an atmosphere. However, the interaction of fragments ejected at escape velocity with the atmosphere leads to their deceleration. It can be approximated that the minimum size of a fragment traversing the atmosphere without substantial deceleration is proportional to the atmospheric pressure (Melosh 1989; Artemieva and Ivanov 2004). Thus, the total escaping mass in a particular impact event depends on the size distribution of the fragments. This distribution may be represented by $N(m) = Cm^{-b}$, where N is the number of fragments with a mass larger than m; and C and b are constants, defined by the total ejected mass and the type of fragmentation: single crushing yields b values between 0.4 and 0.6, whereas a b value of approximately 1 indicates multiple fragmentation (see Melosh 1989, p.91, for details). In the numerical model (Artemieva and Ivanov 2004), this value is substantially higher, at ~2.4, for the largest (and hence, the most interesting) fragments, because only a few really large fragments are usually ejected from a moderately sized crater with escape velocity. If we assume that at a current atmospheric pressure P_0 the fragments with a mass larger than m_0 escape, then the total escaping mass is $M_{esc}^{\,0} \approx N(m_0)m_0$. If the atmospheric pressure is k-times lower, $P_1 = P_0/k$, then the largest escaping fragment is $m_1 = m_0/k^3$ and the total escaping mass is $M_{esc}^{\,1} \approx M_{esc}^{\,0}(1 + k^{3b-3} - k^{-3}) \approx M_{esc}^{\,0}(1 + k^{3b-3})$. Thus, at half the pressure and for a b value of 2.4, the total escaping mass is 19 times larger than at current atmospheric pressure P_0. At a 10 times lower pressure and for the same b value, there is a dramatic increase in escaping material with up to 1.5×10^4 more fragments ejected from the planet. In the case of a shallower slope to the size distribution with b of 0.8–1 and a pressure variation of 0.5 to 0.1 times the current atmospheric pressure P_0, the total mass of escaping material is only 1.5–2 times larger. However, this low value of b is not typical for the largest ejected fragments. Thus, the probability

to launch fragments, which will finally arrive on Earth, is higher for a less dense Martian atmosphere.

A recent ~5 Ma period of low obliquity of Mars, as proposed by Laskar et al. (2004), correlates in time with the increase of the recorded ejection events of Martian meteorites (Fig. 12). Early calculations by Fanale et al. (1982) have indicated that the atmosphere of Mars, which largely consists of carbon dioxide, completely freezes out at the poles at the lowest obliquities, whereas at the highest obliquities, the atmospheric pressure may be significantly higher. According to this model, the atmospheric pressure could vary with changing obliquity between 0.1 and 15 mbar. However, more detailed calculations by Fanale and Salvail (1994) have suggested that the maximum atmospheric pressure never exceeds a value of 1 mbar above the present level, and may be as low as 2 mbar at 10° Martian obliquity. Furthermore, recent calculations by Armstrong et al. (2004) resulted in the conclusion that the atmospheric pressure on Mars remains remarkably constant (with only small variations of <0.5 mbar) because of a strong CO_2-absorption into the surface at high obliquities. Recently, however, sedimentary deposits on the flanks of Tharsis Montes have been interpreted as young glacial deposits in equatorial regions (Márquez et al. 2004). To allow the formation of such glaciers, these authors suggested a warmer climate and a higher atmospheric pressure at 5 to 9 Ma ago.

In summary, the influence of climatic changes on Mars on the atmospheric pressure is still controversial. However, if climatic changes on Mars have a significant influence on the atmospheric pressure, this could account for the observed increase in recorded ejection events of Martian meteorites during the last 5 Ma.

Influence of Local Geology and Morphology

The different CRE ages, indicating 1–3 ejection events of young shergottites with similar crystallization ages of ~170 Ma, have been discussed widely as the Martian meteorite paradox (Gladman 1997; Nyquist et al. 1998; Eugster et al. 2002; Head et al. 2002). Compared to the less than 10% of the surface on Mars that is covered by basaltic provenances younger than 1 Ga (Hartmann and Neukum 2001), the shergottites (representing 72% of all Martian meteorites; Fig. 1) clearly seem to be over-represented in the suite of Martian meteorites.

Possible source regions for the shergottites are Tharsis, Elysium, and Amazonis Planitia, which are all covered partly by young lava flows and share characteristics that could favor impact ejection of surface rocks: These regions are in low latitudes (between 30°N and S latitude). This means that their angular velocity, which on the equator is 0.24 km/sec (equals 5% of the escape velocity), may add energy to the launch process, if it is in the same direction (alternatively, it could be a hindrance, if ejection is in the opposite direction). The young basaltic terrains are commonly elevated more than 5 km above the datum, with the Tharsis bulge rising 10 km above datum. At 10 km above datum, the density of Martian atmosphere is 2.3 times lower and the trajectory length for fragments traversing the atmosphere is substantially shorter. The ejection velocity is higher in the case of impacts into the non-brecciated (young) rocks compared with impacts into regolith-covered old surfaces (Head et al. 2002). As the size of the Martian meteorite source region is only 0.2 R (Artemieva and Ivanov 2004), not only a thick regolith cover but also a glacial cover could reduce the area possibly sampled by the smallest projectiles.

Interplanetary Transfer of Solid Matter

Interplanetary transfer of solid matter from Mars and the Moon has also strong implications for other fields of research, such as the evolution of terrestrial planets and the possible exchange of viable organisms. A potential transfer of organisms in meteorites is supported by low-pressure and low-temperature ejection of Martian meteorites and by new findings in astrobiology (Horneck et al. 2001; Mastrapa et al. 2001).

Assuming that the survival time of meteorites on the surface of Earth is limited to about 1 Ma (Welten et al. 1997, 1999), Armstrong et al. (2002) evaluated the likelihood for preservation of ejected fragments from the terrestrial planets on the surface of the Moon. They concluded that on the lunar surface samples from terrestrial planets originating from the time of the early heavy bombardment 3.9 Ga ago may be found. Estimations for chondritic and terrestrial meteorites on Mars were made by Bland and Smith (2000), who suggested that meteorites could survive on the surface of Mars for approximately 10^9 yr. Additionally, it should be noted that the interplanetary transfer of solid matter is not restricted to the inner solar system. This is inferred from the dark material on the leading side of Saturn's bright moon Iapetus, which is considered to be the result of ejection from the dark moon Phoebe (Hamilton 1997). This documents that the interplanetary transfer of solid matter is an important and a solar-system-wide process.

CONCLUSIONS

Combining the mineralogical observations on Martian meteorites with the results of numerical models of oblique impacts on Mars allows the following conclusions:

1. A p/T range for the launch of Martian surface rocks has been established, with shock pressures recorded between 5 and 55 GPa and the increase of post-shock temperatures ranging from 10 to about 1000 °C.
2. The calculated cooling history in space for the most highly shocked Martian meteorite, ALH 77005, indicates, for a post-shock temperature of 1000 °C, a pre-atmospheric size of about 0.4–0.6 m.

3. The source regions of the Martian meteorites, as defined by numerical simulations (Artemieva and Ivanov 2004), are in good agreement with the burial depth of the subvolcanic to volcanic suite of Martian rocks.
4. The obtained data set suggests, on average, a shorter travel time for more strongly shocked fragments.
5. Climatic change, namely variation of atmospheric pressure, may influence the ejection of Martian meteorites. However, the variability of Martian climate is still debated.
6. Some of the Martian meteorites were subjected to relatively low shock pressures and post-shock temperature elevation. This observation renders the possibility of ejection of potentially viable organisms in Martian surface rocks possible.

Acknowledgments–We thank H. Schneider and H. Schick for the construction of the heating stage used for the refractive index measurements, and H.-R. Knöfler for sample preparation. Constructive comments by Richard Grieve, two anonymous reviewers, and the Associate Editor Uwe Reimold improved the quality of the paper and are very much appreciated. The authors gratefully acknowledge the generous supply of the samples by the Natural History Museum, London, the NASA Meteorite Working Group, the Museum National d'Historie Naturelle, Paris, the Max-Planck-Institut für Chemie, Mainz, the Institute of Geophysics and Planetary Physics, Los Angeles, the National Institute of Polar Research, Tokyo, and the finder of DaG 476. This work was partly supported by the DFG-Projects GR-1658 and 436 RUS 17/32/03.

Editorial Handling—Dr. Wolf Uwe Reimold

REFERENCES

Armstrong J. C., Wells E. L., and Gonzales G. 2002. Rummaging through Earth's attic for remains of ancient life. *Icarus* 160:183–196.

Armstrong J. C., Leovy C. B., and Quinn T. 2004. A 1 Gyr climate model for Mars: New orbital statistics and the importance of seasonally resolved polar processes. *Icarus* 171:255–271.

Artemieva N. and Shuvalov V. V. 2001. Extraterrestrial material deposition after the impacts into continental and oceanic sites. In *Geological and biological effects of impact events*, edited by Buffetaut E. and Koeberl C. Berlin: Springer. pp. 249–263.

Artemieva N. and Ivanov B. A. 2002. Ejection of Martian meteorites: Can they fly? (abstract #1113). 33rd Lunar and Planetary Science Conference. CD-ROM.

Artemieva N. and Ivanov B. A. 2004 Launch of Martian meteorites in oblique impacts. *Icarus* 171:84–101.

Badjukov D. D., Nazarov M. A., and Taylor L. A. 2001. Shock metamorphism in the shergottite meteorite Dhofar 019 (abstract #2195). 32nd Lunar and Planetary Science Conference. CD-ROM.

Bauer J. F. 1979. Experimental shock metamorphism of mono- and polycrystalline olivine—A comparative study. Proceedings, 10th Lunar and Planetary Science Conference. pp. 2573–2596.

Baker V. R. 2001. Water and the Martian landscape. *Nature* 412:228–236.

Beck P., Gillet P., Gautron L., Daniel I. and El Goresy A. 2004. A new natural high-pressure (Na, Ca)-hexaluminosilicate [$(Ca_xNa_{1-x})Al_{3+x}Si_{3-x}O_{11}$] in shocked Martian meteorites. *Earth and Planetary Science Letters* 219:1–12.

Bischoff A. and Stöffler D. 1992. Shock metamorphism as a fundamental process in the evolution of planetary bodies: Information from meteorites. *European Journal of Mineralogy* 4: 707–755.

Bland P. A. and Smith T. B. 2000. Meteorite accumulations on Mars. *Icarus* 144:21–26.

Borg L. E., Nyquist L. E., Reese Y., Wiesmann H., Shih C.-Y., Ivanova M., Nazarov M. A., and Taylor L. A. 2001. The age of Dhofar 019 and its relationship to the other Martian meteorites (abstract #1144). 32nd Lunar and Planetary Science Conference. CD-ROM.

Chao E. C. T., Shoemaker E. M., and Madsen B. M. 1960. First natural occurrence of coesite. *Science* 132:220–222.

Chen M., Sharp T. G., El Goresy A., Wopenka B., and Xie X. D. 1996. The majorite-pyrope plus magnesiowüstite assemblage: Constraints on the history of shock melt veins in chondrites. *Science* 271:1570–1573.

Dodd R. T. and Jarosewich E. 1979. Incipient melting in and shock classification of L-group chondrites. *Earth and Planetary Science Letters* 44:335–340.

Dworak U. 1969. Stoßwellenmetamorphose des Anorthosits vom Manicouagan Krater, Quebec, Canada. *Contributions to Mineralogy and Petrology* 24:306–347.

Engelhardt W., V., Arndt J., Stöffler D., Müller W. F., Jeziorkowski H., and Gubser R. A. 1967. Diaplektische Gläser in den Breccien des Ries von Nördlingen als Anzeichen für Stoßwellenmetamorphose. *Contributions to Mineralogy and Petrology* 15:93–102.

Eugster O., Busemann H., Lorenzetti S., and Terribilini D. 2002. Ejection ages from krypton-81-krypton-83 dating and pre-atmospheric sizes of Martian meteorites. *Meteoritics & Planetary Science* 37:1345–1360.

Fanale F. P. and Salvail J. R. 1994. Quasi-periodic atmosphere-regolith-cap CO_2 redistribution in the Martian past. *Icarus* 111: 305–316.

Fanale F. P., Salvail J. R., Banerdt W. B., Saunders R. S., and Johansen L. A. 1982. Seasonal carbon dioxide exchange between the regolith and atmosphere of Mars—Experimental and theoretical results. *Journal of Geophysical Research* 87:10,215–10,225.

Fritz J., Greshake A., and Stöffler D. 2004. Micro-Raman spectroscopy of plagioclase and maskelynite in Martian meteorites: Evidence of progressive shock metamorphism (abstract). *Antarctic Meteorites* 28:10–11.

Fritz J., Greshake A., and Stöffler D. 2005. Micro-Raman spectroscopy of plagioclase and maskelynite in Martian meteorites: Evidence of progressive shock metamorphism. *Antarctic Meteorite Research* 18:96–116.

Fritz J., Greshake A., Hecht L., and Stöffler D. 2002. Shock metamorphism of Martian meteorites: New data from quantitative shock barometry (abstract #1504). 33rd Lunar and Planetary Science Conference. CD-ROM.

Gibbons R. V. and Ahrens T. J. 1977. Effects of shock pressure on calcic plagioclase. *Physics and Chemistry of Minerals* 1:95–107.

Garrison D. H., Rao M. N., and Bogard D. D. 1995. Solar-proton-produced neon in shergottite meteorites and implications for their origin. *Meteoritics* 30:738–747.

Gladman B. 1997 Destination: Earth. Martian meteorite delivery. *Icarus* 130:228–246.

Gnos E., Hofmann B., Franchi I. A., Al-Kathiri A., Hauser M., and Moser L. 2002. Sayh al Uhaymir 094: A new Martian meteorite from the Oman desert. *Meteoritics & Planetary Science* 37:835–854.

Greenwood J. P. and McSween H. Y., Jr. 2001. Petrogenesis of Allan Hills 84001: Constrains from impact-melted feldspathic and silica glasses. *Meteoritics & Planetary Science* 36:43–61.

Greshake A., Fritz J., and Stöffler D. 2004. Petrology and shock metamorphism of the olivine-phyric shergottite Yamato-980459: Evidence for a two stage cooling and a single-stage ejection history. *Geochimica et Cosmochimica Acta* 68:2359–2377.

Hamilton D. P. 1997. Iapetus: 4.5 billion years of contamination by Phoebe dust (abstract). *Bulletin of the American Astronomical Society* 29:1010.

Hartman W. K. and Neukum G. 2001. Crater chronology and the evolution of Mars. *Space Science Reviews* 96:165–196.

Head J. N., Melosh H. J., and Ivanov B. A. 2002. Martian meteorite launch: High-speed ejecta from small craters. *Science* 298:1752–1756.

Head J. W., Mustard J. F., Kreslavsky M. A., Milliken R. E., and Marchant D. R. 2003. Recent ice ages on Mars. *Nature* 426:797–802.

Heider N. and Kenkmann T. 2003. Numerical simulation of temperature effects at fissures due to shock loading. *Meteoritics & Planetary Science* 38:1451–1460.

Hofmeister A. M. 1999. Mantle values of thermal conductivity and geotherm from Phonon lifetimes. *Science* 283:1699–1706.

Horneck G., Stöffler D., Eschweiler U., and Hornemann U. 2001. Bacterial spores survive simulated meteorite impact. *Icarus* 149: 285–290.

Jarosewich E., Nelen J. A., and Norberg J. A. 1980. Reference samples for electron microprobe analysis. *Geostandard Newsletters* 4:43–47.

Jarosewich E., Gooley R., and Hussler J. 1987. Chromium augite—A new microprobe reference sample. *Geostandard Newsletters* 11:197–198.

Jull A. J. T. and Donahue D. J. 1988. Terrestrial ^{14}C age of the Antarctic shergottite EET A79001. *Geochimica et Cosmochimica Acta* 52:1309–1311.

Jull A. J. T., Cielaszyk E, Brown S. T., and Donahue D. J. 1994. ^{14}C terrestrial age of achondrites from Victoria Land, Antarctica. (abstract). 25th Lunar and Planetary Science Conference. pp. 647–648.

Jull A. J. T., Klandrud S. E., Schnabel C., Herzog G. F., Nishiizumi K., and Caffee M. W. 1999. Cosmogenic radionuclide studies of the nakhlites (abstract #1004). 30th Lunar and Planetary Science Conference. CD-ROM.

Kenkmann T., Hornemann U., and Stöffler D. 2000. Experimental generation of shock-induced pseudotachylites. *Meteoritics & Planetary Science* 35:1275–1290.

Kleber W. 1970. *An introduction to crystallography.* Berlin: VEB Verlag Technik. 366 pp.

Koizumi E., McKay G., Mikouchi T., Le L., Schwandt C., Monkawa A., and Miyamoto M. 2002. Crystallization experiments of the Martian meteorite QUE 94201: Additional constraints on its formation condition (abstract #1442). 33rd Lunar and Planetary Science Conference. CD-ROM.

Lambert P. 1985. Metamorphic record in shergottites (abstract). *Meteoritics* 20:A690.

Langenhorst F. and Poirier J.-P. 2000. Anatomy of black veins in Zagami: Clues to the formation of high-pressure phases. *Earth and Planetary Science Letters* 184:37–55.

Langenhorst F., Stöffler D., and Klein D. 1991. Shock metamorphism of the Zagami achondrite (abstract). 20th Lunar and Planetary Science Conference. pp. 779–780.

Laskar J., Levrard B. and Mustard J. F. 2002 Orbital forcing of the Martian polar layered deposits. *Nature* 419:375–377.

Laskar J., Correia A. C. M., Gastineau M., Joutel F., Levrard B., and Robutel P. 2004. Long term evolution and chaotic diffusion of the insolation quantities of Mars. *Icarus* 170:343–364.

Leroux H. 2001. Microstructural shock signatures of major minerals in meteorites. *European Journal of Mineralogy* 13:253–272.

Lodders K. and Fergley B. 1998. *The planetary scientist's companion.* Oxford: Oxford University Press. 371 p.

Lu R., Hofmeister A. M., and Wang Y. 1994. Thermodynamic properties of ferromagnesium silicate perovskites from vibrational spectroscopy. *Journal of Geophysical Research* 99: 11,795–11,804.

Mastrapa R. M. E., Glanzberg H., Head J. N., Melosh H. J., and Nicholson W. L. 2001. Survival of bacteria exposed to extreme acceleration: Implications for panspermia. *Earth and Planetary Science Letters* 189:1–8.

Márquez Á., Fernández C., Anguita F., Farelo A., Anguita J., and De La Casa M.-Á. 2004. New evidence for a volcanically, tectonically, and climatically active Mars. *Icarus* 172:573–581.

McCoy T. J. and Lofgren G. E. 1999. Crystallization of the Zagami shergottite: An experimental study. *Earth and Planetary Science Letters* 173:397–411.

McCoy T. J., Taylor G. J., and Keil K. 1992. Zagami—Product of a two-stage magmatic history. *Geochimica et Cosmochimica Acta* 56:3571–3582.

McSween H. Y., Jr. 2002. The rocks of Mars, from far and near. *Meteoritics & Planetary Science* 37:7–25.

McSween H. Y., Jr. and Stolper E. 1980. Basaltic meteorites. *Scientific American* 242:54–63.

Melosh H. J. 1984. Impact ejection, spallation, and the origin of meteorites. *Icarus* 59:234–260.

Melosh H. J. 1989. *Impact cratering: A geologic process.* Oxford: Oxford University Press. 246 p.

Meyer C. 2004. Mars meteorite compendium. http://curator.jsc.nasa.gov/curator/antmet/mmc/mmc.htm. Accessed on September 16, 2005.

Mikouchi T. and Miyamoto M. 2000. Lherzolitic Martian meteorites Allan Hills 77005, Lewis Cliff 88516, and Yamato-793605: Major and minor element zoning in pyroxene and plagioclase glass. *Antarctic Meteorite Research* 13:256–269.

Mikouchi T. and Miyamoto M. 2002. Comparative cooling rates of nakhlites as inferred from iron-magnesium and calcium zoning of olivines (abstract #1343). 33rd Lunar and Planetary Science Conference. CD-ROM.

Mikouchi T. and McCay G. A. 2003. Shock heating and subsequent cooling of basaltic shergottites: The case for QUE 94201 and Dhofar 378 (abstract #1920). 34th Lunar and Planetary Science Conference. CD-ROM.

Mikouchi T., Miyamoto M., and McKay G. A. 2001. Mineralogy and petrology of the Dar al Gani 476 Martian meteorite: Implications for its cooling history and relationship to other shergottites. *Meteoritics & Planetary Science* 36:531–548.

Mikouchi T., Koizumi E., McKay G. A., Monkawa A., Ueda Y., and Miyamoto M. 2003. Mineralogy and petrology of Yamato-000593: Comparison with other Martian nakhlite meteorites. *Antarctic Meteorite Research* 16:34–57.

Milton D. J. and Decarli P. S. 1963. Maskelynite: Formation by explosive shock. *Science* 140:670–671.

Misawa K., Shih C.-Y., Wiesmann H., and Nyquist L. E. 2003. Crystallization and alteration ages of the Antarctic nakhlite Yamato-000593 (abstract #1556). 34th Lunar and Planetary Science Conference. CD-ROM.

Monkawa A., Mikouchi T., Koizumi E., Chokai J., and Miyamoto M. 2004. Fast cooling history of the Chassigny Martian meteorite

(abstract #1535). 35th Lunar and Planetary Science Conference. CD-ROM.

Müller W. F. 1993. Thermal and deformation history of the Shergotty meteorite deduced from clinopyroxene microstructure. *Geochimica et Cosmochimica Acta* 57:4311–4322.

Mustard J. F., Cooper C. D., and Rifkin M. K. 2001. Evidence for recent climate change on Mars from the identification of youthful near-surface ground ice. *Nature* 412:411–414.

Nagao K., Nakamura T., Miura Y. N., and Takaoka N. 1997. Noble gases and mineralogy of primary igneous materials of the Yamato-793605 shergottite. *Antarctic Meteorite Research* 10: 125–142.

Nishiizumi K. and Caffee W. 1996. Exposure history of shergottite Queen Alexandra Range 94201 (abstract). 27th Lunar and Planetary Science Conference. pp. 961–962.

Nishiizumi K. and Hillegonds D. J. 2004. Exposure and terrestrial history of new Yamato, lunar, and Martian meteorites (abstract). *Antarctic Meteorites* 28:60–61.

Nishiizumi K., Klein J., Middleton R., Elmore D., Kubik P. W., and Arnold J. R. 1986. Exposure history of shergottites. *Geochimica et Cosmochimica Acta* 50:1017–1021.

Nishiizumi K., Okazaki R., Park J., Nagao K., Masarki J., and Finkel R. C. 2002. Exposure and terrestrial histories of Dhofar 019 Martian meteorite (abstract #1366). 33rd Lunar and Planetary Science Conference. CD-ROM.

Nyquist L. E. 1982. Do oblique impacts produce Martian meteorites (abstract)? 13th Lunar and Planetary Science Conference. pp. 602–603.

Nyquist L. E., Borg L. E., and Shih C.-Y. 1998. The shergottite age paradox and the relative probabilities for Martian meteorites of differing ages. *Journal of Geophysical Research* 12:31,445–31,456.

Nyquist L. E., Bogard D. D., Shih C.-Y., Greshake A., Stöffler D,. and Eugster O. 2001. Ages and history of Martian meteorites. *Space Science Reviews* 96:105–164.

Nyquist L.E., Bogard D. D., Wooden J. L., Wiesmann H., Shin C.-Y., Bansae B. M., and McKay G. 1979. Early differentiation, late magmatism, and recent bombardment on the shergottite parent planet (abstract). *Meteoritics* 14:502.

Okazaki R., Nagao K., Imae N., and Kojima H. 2003. Noble gas signatures of Antarctic nakhlites, Yamato-000593, Y-000749, and Y-000802. *Antarctic Meteorite Research* 16:58–79.

O'Keefe J. D. and Ahrens T. J. 1983. Constraints on the impact-on-Mars origin of SNC meteorites (abstract). 14th Lunar and Planetary Science Conference. pp. 578–579.

O'Keefe J. D. and Ahrens T. J. 1986. Oblique impact: A process for obtaining meteorite samples from other planets. *Science* 234: 346–349.

Ostertag R. 1982. Annealing behavior of diaplectic plagioclase glass (abstract). Proceedings, 13th Lunar and Planetary Science Conference. pp. 607–608.

Ostertag R. 1983. Shock experiments on feldspar crystals. *Journal of Geophysical Research* 88:B364–376.

Pierazzo E. and Melosh H. J. 2000. Hydrocode modeling of oblique impacts: The fate of the projectile. *Meteoritics & Planetary Science* 35:117–130.

Reimold W. U. and Stöffler D. 1978. Experimental shock metamorphism of dunite. Proceedings, 9th Lunar and Planetary Science Conference. pp. 2805–2824.

Schmitt R. T. 2000. Shock experiments with the H6 chondrite Kernouvè: Pressure calibration of microscopic shock effects. *Meteoritics & Planetary Science* 35:545–560.

Schwenzer S. P. 2004. Marsmeteorite: Edelgase in Mineralseparaten, Gesamtgestein und terrestrischen Karbonaten. Ph.D. thesis, Johannes-Gutenberg-Universität, Mainz, Germany.

Schwenzer S. P., Fritz J., Greshake A., Herrmann S., Jochum K. P., Ott U., Stöffler D., and Stoll B. 2004. Helium loss and shock pressures in Martian meteorites—A relationship (abstract). *Meteoritics & Planetary Science* 39:A96.

Sharp T. G., El Goresy A., Wopenka B., and Chen M. 1999. A post-stishovite SiO_2 polymorph in the meteorite Shergotty: Implications for impact events. *Science* 284:1511–1513.

Shih C. E., Nyquist L. E., and Wiesmann H. 2003. Isotopic studies of Antarctic olivine-phyric shergottite Y-980459 (abstract). Symposium, Evolution of Solar System Materials: A New Perspective from Antarctic Meteorites. pp. 125–126.

Shukolyukov Y. A., Nazarov M. A., and Schultz L. 2000. Dhofar 019: A shergottite with an approximately 20-million-year exposure age (abstract). *Meteoritics & Planetary Science* 35:A147.

Shuvalov V. V. 1999. Multidimensional hydrodynamic code SOVA for interfacial flows: Application to the thermal layer effect. *Shock Waves* 9:381–390.

Stöffler D. 1967. Deformation und Umwandlung von Plagioklas durch Stoßwellen in den Gesteinen des Nördlinger Ries. *Contributions to Mineralogy and Petrology* 16:51–83.

Stöffler D. 1974. Deformation and transformation of rock-forming minerals by natural and experimental shock processes. *Fortschritte der Mineralogie* 51:256–289.

Stöffler D. 1982. Density of minerals and rocks under shock compression. In *Landolt-Börnstein—Numerical data and functional relationships in science and technology,* edited by Angenheister G. Berlin: Springer. pp. 120–183.

Stöffler D. and Hornemann U. 1972. Quartz and feldspar glasses produced by natural and experimental shock. *Meteoritics* 7:371–394.

Stöffler D. and Langenhorst F. 1994. Shock metamorphism of quartz in nature and experiment: I. Basic observation and theory. *Meteoritics* 29:155–188.

Stöffler D., Keil K. and Scott E. R. D. 1991. Shock metamorphism of ordinary chondrites. *Geochimica et Cosmochimica Acta* 55: 3845–3867.

Stöffler D., Ostertag R., Jammes C., Pfannschmidt G., Sen Gupta P. R., Simon S. B., Papike J. J., and Beauchamp R. H. 1986. Shock metamorphism and petrography of the Shergotty achondrite. *Geochimica et Cosmochimica Acta* 50:889–903.

Swift H. F. and Clark B. C. 1983. Mechanism for crater debris escape from planetary-sized bodies (abstract). 14th Lunar and Planetary Science Conference. pp. 765–766.

Swindle T. D., Li B., and Kring D. A. 1996. Noble gases in Martian meteorite QUE 94201 (abstract). 27th Lunar and Planetary Science Conference. pp. 1297–1298.

Szymanski A., Brenker F. E., El Goresy A., and Palme H. 2003. Complex thermal history of Nakhla and Y-000593 (abstract). 34th Lunar and Planetary Science Conference. CD-ROM.

Taylor L. A., Nazarov M. A., Shearer C. K., McSween H. Y., Jr., Cahill J., Neal C. R., Ivanova M. A., Barsukova L. D., Lentz R. C., Clayton R. N., and Mayeda T. K. 2002. Martian meteorite Dhofar 019: A new shergottite. *Meteoritics & Planetary Science* 37:1107–1128.

Thompson S. L. and Lauson H. S. 1972. *Improvements in the chart D radiation-hydrodynamic code III: Revised analytical equation of state.* Albuquerque: Sandia National Laboratory Report #SC-RR-61 0714. 119 p.

Treiman A. H. 1998. The history of Allan Hills 84001 revised: Multiple shock events. *Meteoritics & Planetary Science* 33:753–764.

Tröger W. E. 1982. *Optische Bestimmung der gesteinsbildenden Minerale. Teil 1 Bestimmungstabellen.* Stuttgart: Schweizerbart. 188 p.

Trunin R. F., Gudarenko L. F., Zhernokletov M. V., and Simakov G. V. 2001. *Experimental data on shock compression and*

adiabatic expansion of condensed matter. Sarov: Russian Federal Nuclear Center. 446 p.

Tschermak G. 1872. Die Meteoriten von Shergotty and Gopalpur. Wien: *Sitzungsbericht der Kaiserlichen Akademie der Wissenschaften* 65:122–146.

Vickery A. M. and Melosh H. J. 1987. The large crater origin of SNC meteorites. *Science* 237:738–743.

Walker D., Stolper E. M., and Hays J. F. 1979. Basaltic volcanism: The importance of planet size. Proceedings, 10th Lunar and Planetary Science Conference. pp. 1995–2015.

Waples D. W. and Waples J. S. 2004. A review and evaluation of specific heat capacities of rocks, minerals and subsurface fluids. Part 1: Minerals and non-porous rocks. *Natural Resources Research* 13:97–122.

Ward W. R. 1974. Climatic variations on Mars 1: Astronomical theory of insolation. *Journal of Geophysical Research* 79:3375–3386.

Warren P. 1994. Lunar and Martian meteorites delivery services. *Icarus* 111:338–363.

Wasson J. T. and Wetherill G. W. 1979. Dynamical, chemical and isotopic evidence regarding the formation locations of asteroids and meteorites. In *Asteroids*, edited by Gehrels T. Tucson, Arizona: The University of Arizona Press. pp. 926–974.

Weiss B. P., Kirschvink J. L., Baudenbacher F. J., Vali H., Peters N. T., MacDonald F. A., and Wikswo J. P. 2000. A low temperature transfer of ALH 84001 from Mars to Earth. *Science* 290:791–795.

Welten K. C., Alderliesten C., Van der Borg K., Lindner L., Loeken T., and Schultz L. 1997. Lewis Cliff 86360, an Antarctic L chondrite with a terrestrial age of 2.35 million years. *Meteoritics & Planetary Science* 32:775–780.

Welten C. K., Lindner L., Alderliesten C., and Van der Borg K. 1999. Terrestrial ages of ordinary chondrites from the Lewis Cliff standing area, East Antarctica. *Meteoritics & Planetary Science* 34:559–569.

Wetherill G. W. 1984. Orbital evolution of impact ejecta from Mars. *Meteoritics* 19:1–13.

Wood C. A. and Ashwal L. D. 1981. Meteorites from Mars: Prospects, problems, and implications (abstract). 12th Lunar and Planetary Science Conference. pp. 1197–1199.